

## Supplementary Information

### Manuscript title: Leiomodin-3 is essential for thin filament organization in skeletal muscle

#### Supplementary Methods

##### Analysis of *LMOD3* variants

*LMOD3* variants identified in NM patients were analyzed according to their predicted effect on Lmod3 protein and their presence in two large control databases including the Exome Variant Server, NHLBI GO Exome Sequencing Project (ESP), Seattle, WA (<http://evs.gs.washington.edu/EVS/>) and the 1000 Genomes database (1), both of which were accessed in June 2014 and which together contain exome sequence data from over 7000 individuals from a wide range of ethnic backgrounds without known genetic muscle disorders. Polyphen2 (<http://genetics.bwh.harvard.edu/pph2/>) and SIFT (<http://sift.jcvi.org/>) pathogenicity prediction programs were used to perform in silico analysis of missense variants.

##### Analysis of clinical and histological features of *LMOD3*-NM patients

Information on clinical features in affected individuals and images of light and electron microscopy from skeletal muscle biopsy of these patients was reviewed and collated. The frequency of each clinical feature was calculated based on the number of patients for which data was available.

##### Expression of recombinant Leiomodin full length and N-terminal fragments for antibody (Ab) testing

###### *cDNA expression constructs*

The cDNA encoding full length *LMOD2* (AK300698.1), full length *LMOD3* (NM\_198271) and C-terminal truncations (200X, 100X and 51X) of *LMOD3* were PCR amplified from an *LMOD2* construct (provided as a gift courtesy of Roberto Dominguez, University of Pennsylvania, Philadelphia as described in (2)) and an *LMOD3* construct (obtained from SourceBioscience, IMAGE BC121019). Primer sequences are available upon request. Amplicons were cloned into the *Xma*I/*Sa*lI sites of pGEX2T(new), a multiple cloning site (MCS) modified version of pGEX2T vector, that expresses an inserted sequence with an N-terminal in-frame GST-tag. The inserts were subcloned into the *Xma*I/*Sa*lI sites of pMT3-FLAGc, a modified version of the pMT2 vector with a FLAG sequence and a modified MCS vector that expresses inserted sequences with an N-terminal in-frame FLAG tag. All constructs were fully sequenced to check fidelity.

###### *Bacterial expression of GST-tagged protein and GST purification*

The pGEX2T(new) constructs and the empty vector which expresses GST-only were transformed into competent BL21 strain bacteria and inoculated 10 mL LB<sub>amp</sub> cultures were incubated for 5 hr at 37°C. 0.2 mM IPTG was added to induce protein expression and cultures were incubated for a further 2 hr at 37°C. Pelleted bacteria were re-suspended in PBS with 1% Triton X100, 1 mM DTT and 1x PI cocktail, sonicated and centrifuged and the GST-fusion proteins from the supernatants were purified using GST SpinTrap columns (GE Healthcare, 28-9523-59) following manufacturer's instructions. SDS-PAGE sample buffer was added to supernatants.

###### *Mammalian expression of FLAG-tagged protein*

Two µg of DNA for each of the pMT3-FLAGc constructs, including empty vector and a pMT3-FLAGc-ACTN2 construct as negative controls for the Lmod3 Ab characterization, were transfected into 10 cm dishes of 15% confluent mammalian COS-1 cells using X-tremeGENE 9 transfection reagent (Roche, 06 365 787 001) following manufacturer's instructions. Cells were incubated at 37°C/5% CO<sub>2</sub>, for 42 hr. Cells were washed with PBS and scraped off the dishes and pelleted. The pellets were re-suspended in 250 µL NP40 lysis buffer (50 mM Tris, pH 8.0, 150 mM NaCl, 1% NP40, 0.2 mM PMSF, 1x PI cocktail), incubated on ice for 30 min, centrifuged and SDS-PAGE sample buffer was added to the supernatants.

##### Antibody staining of stretched fiber bundles isolated from frozen biopsies

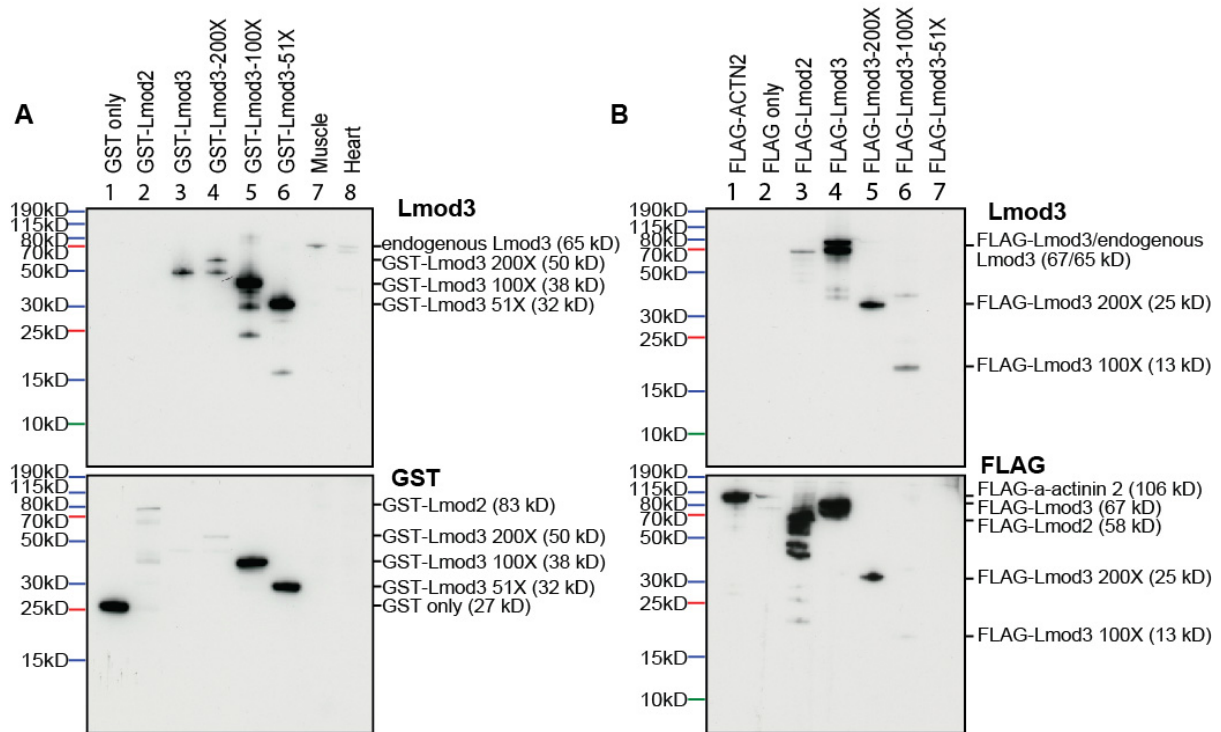
For confocal imaging small aluminum clips were glued to a glass slide. Fiber bundles from frozen biopsies were stretched and fixed between the aluminum clips in relaxing buffer with protease

inhibitors. Stretched bundles were then fixed using 3% para-formaldehyde (PFA) in PBS for 20 min at 4°C, followed by washes in PBS (five buffer changes, last wash over night at 4°C).

For immunolabelling (co-staining with Tmod/ $\alpha$ -actinin/phalloidin) bundles were fixed and washed as described above, followed by blocking in 4% BSA, 0.01% Triton in PBS for 2 hr at 4°C. Primary Ab (Tmod and  $\alpha$ -actinin) and Alexa488-Phalloidin were diluted in 4% BSA in PBS and incubated on preparations for 24 hr at 4°C. Primary antibody was removed by washing 4 times 5 min in PBS followed by 30 min blocking in 4% BSA. Bundles were incubated in secondary antibody and Alexa488-Phalloidin diluted in blocking solution for 24hr. Unbound antibody was removed by washing as above followed by mounting in Vectorshield with #0 coverslips.

Staining was analyzed by confocal microscopy and thin filament length was measured using Image J (Version 1.44, Wayne Rasband, National Institutes of Health, <http://rsbweb.nih>).

## Supplementary Figures



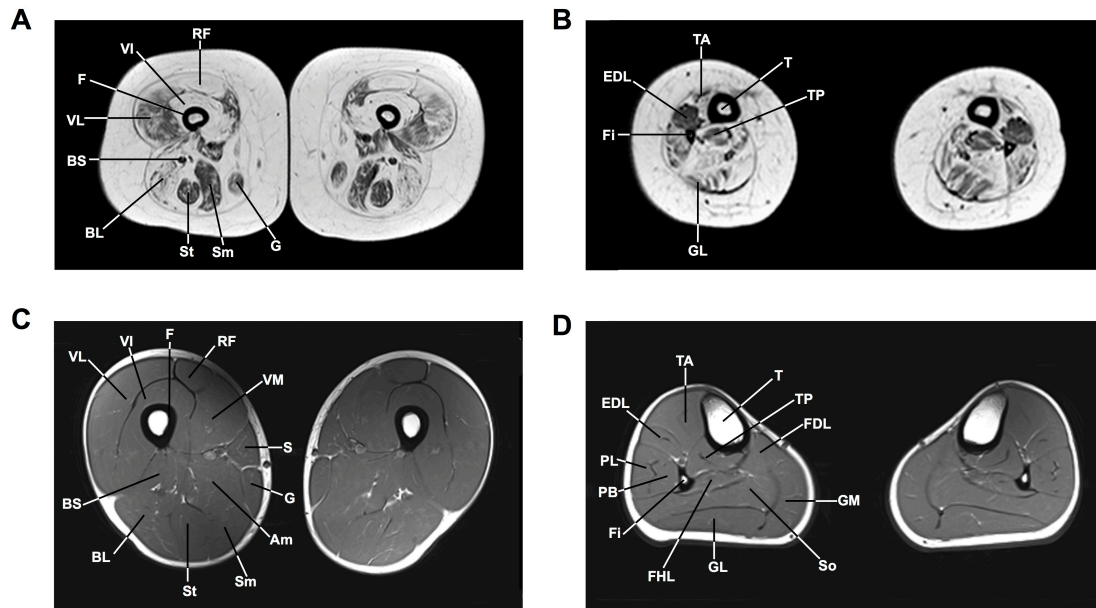
### Supplementary Figure 1: The leiomodinin-3 (Lmod3) Ab recognizes N-terminal Lmod3 fragments as short as 51 amino acids in length

Equal amounts of **(A)** bacterially expressed GST-fusion proteins and **(B)** mammalian cell expressed FLAG-fusion proteins were run on replicate 10% Bis-Tris gels in MES buffer. For the bacterially expressed proteins 1/50<sup>th</sup> of the amount was loaded for the Lmod3 Ab gel compared to the GST Ab gel. **(A)** 10 µg of human skeletal muscle and mouse heart lysates served as positive controls for the Lmod3 Ab.

**(A)** Full length GST-Lmod3 could not be expressed in bacteria (no band at the predicted size of 92kD on the GST and Lmod3 blots, lane 3). The Lmod3 Ab detects endogenous Lmod3 in human skeletal muscle (lane 7) and mouse heart (lane 8). GST-Lmod3 N-terminal fragments, 200X, 100X and 51X were expressed in bacteria and were detected by both the GST and Lmod3 Ab. Lmod3 Ab did not detect the GST-tag alone (lane 1). Full length GST-Lmod2 was expressed at low levels in bacteria and is detected by the GST Ab (lane 2) but not by the Lmod3 Ab.

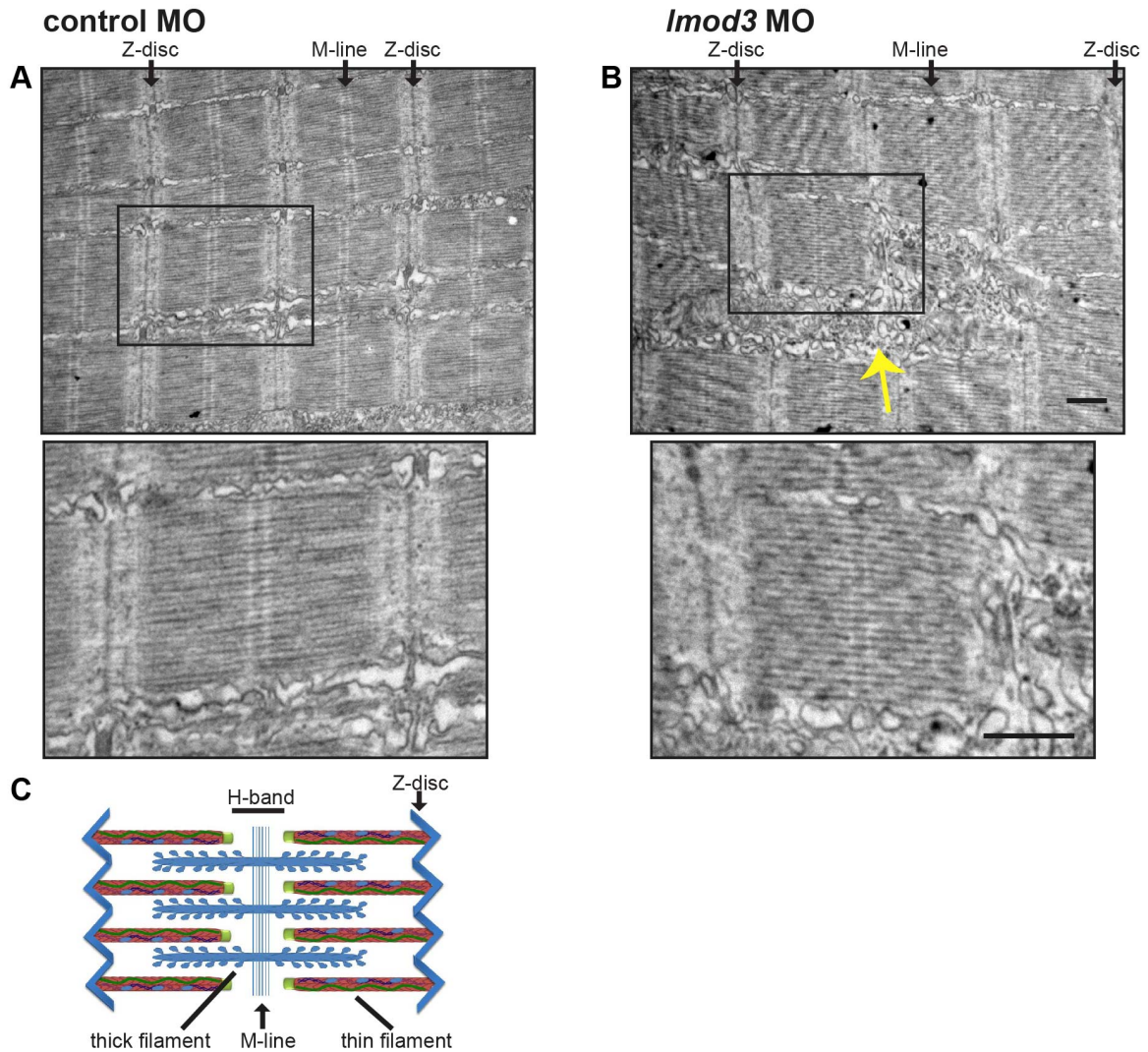
**(B)** Full length FLAG-Lmod3 and, to a lesser extent, the 200X and 100X truncations of Lmod3 were expressed in mammalian cells, as demonstrated by bands of approximately the expected sizes on blots probed with FLAG (bottom panel) and Lmod3 Ab (top panel). The FLAG-Lmod3 51X protein was not expressed in COS cells (not detected with FLAG or Lmod3 Ab, lane 7). FLAG-α-actinin 2 was not detected by the Lmod3 Ab, suggesting no cross-reactivity with the tag or α-actinin 2. However, Lmod3 Ab did cross-react weakly with highly concentrated FLAG-Lmod2 protein (Lane 3). In the mammalian cell expression system the FLAG-Lmod2 and FLAG-Lmod3 constructs all ran at a larger size than the predicted molecular weight, possibly due to post-translational modifications added in mammalian cells. GST Ab were purchased from Roche (27-4577-01, goat Ab, at 1:1000) and FLAG Ab from Sigma (F1804, mouse Ab, at 1:500).

In summary, a protein fragment comprised of 51 N-terminal amino acids of Lmod3 (expressed in bacterial cells) as well as N-terminal fragments 100 and 200 amino acids long (expressed in bacterial and mammalian cells) were specifically detected by the Lmod3 Ab. Lmod3 Ab weakly cross-reacted with full length Lmod2.



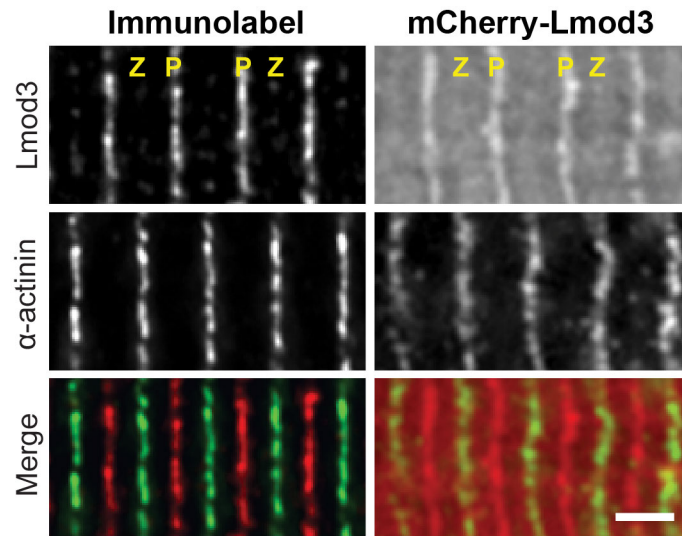
### Supplementary Figure 2: Lower limb muscle involvement in *LMOD3*-NM

T1-weighted MRI images from Patient 14a, at age 9 years showing transverse sections of the proximal thigh (**A**) and proximal lower leg (**B**). T1-weighted MRI images from the proximal thigh (**C**) and proximal lower leg (**D**) of a 17 year old healthy male are shown for comparison. MRI images in Patient 14a show diffuse involvement of thigh and lower leg muscles with marked generalised atrophy and symmetrical fatty infiltration of most muscles. There is relative sparing of the short head of biceps femoris (BS) and gracilis (G) muscles (see Panel **A**) and of tibialis anterior (TA) and extensor digitorum longus (EDL) (see panel **B**). BL, biceps femoris long head; BS, biceps femoris short head; EDL, extensor digitorum longus; EHL, extensor hallucis longus; F, femur; FDL, flexor digitorum longus; FHL, flexor hallucis longus; Fi, fibula; G, gracilis; GM, gastrocnemius medialis; GL, gastrocnemius lateralis; PB, peroneus brevis; PL, peroneus longus; RF, rectus femoris; S, sartorius; Sm, semimembranosus; So, soleus; St, semitendinosus; T, tibia; TA, tibialis anterior; TP, tibialis posterior; VI, vastus intermedius; VL, vastus lateralis; VM, vastus medialis.



**Supplementary Figure 3: Electron microscopy of morpholino *lmod3* knock-down zebrafish demonstrates abnormalities around the M-line**

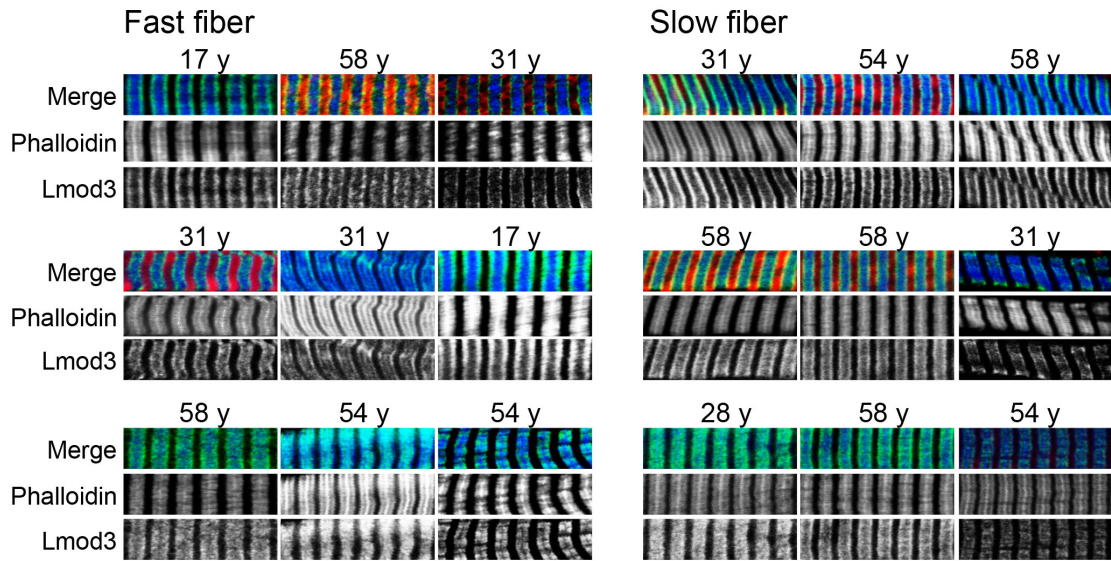
(A, B) Electron micrographs of skeletal muscle from control (left) and *lmod3* MO zebrafish (right) are shown (same magnification). General sarcomeric structure is preserved, but intramyofibrillar spaces are enlarged (yellow arrow) in *lmod3* MO zebrafish and non-specific abnormalities are seen around the M-line. This could represent either loss of the H-band border, which relies on well-aligned thin filament pointed ends, as illustrated in the schematic of the sarcomere (C) or disruption to the myosin thick filaments. Sarcomere length was  $\sim 1.7 \mu\text{m}$  in both control and *lmod3* MO zebrafish. Scale bar (B) 500nm (corresponds to both upper and lower panels).



**Supplementary Figure 4: Localization of Lmod3 in cultured quail myotubes**

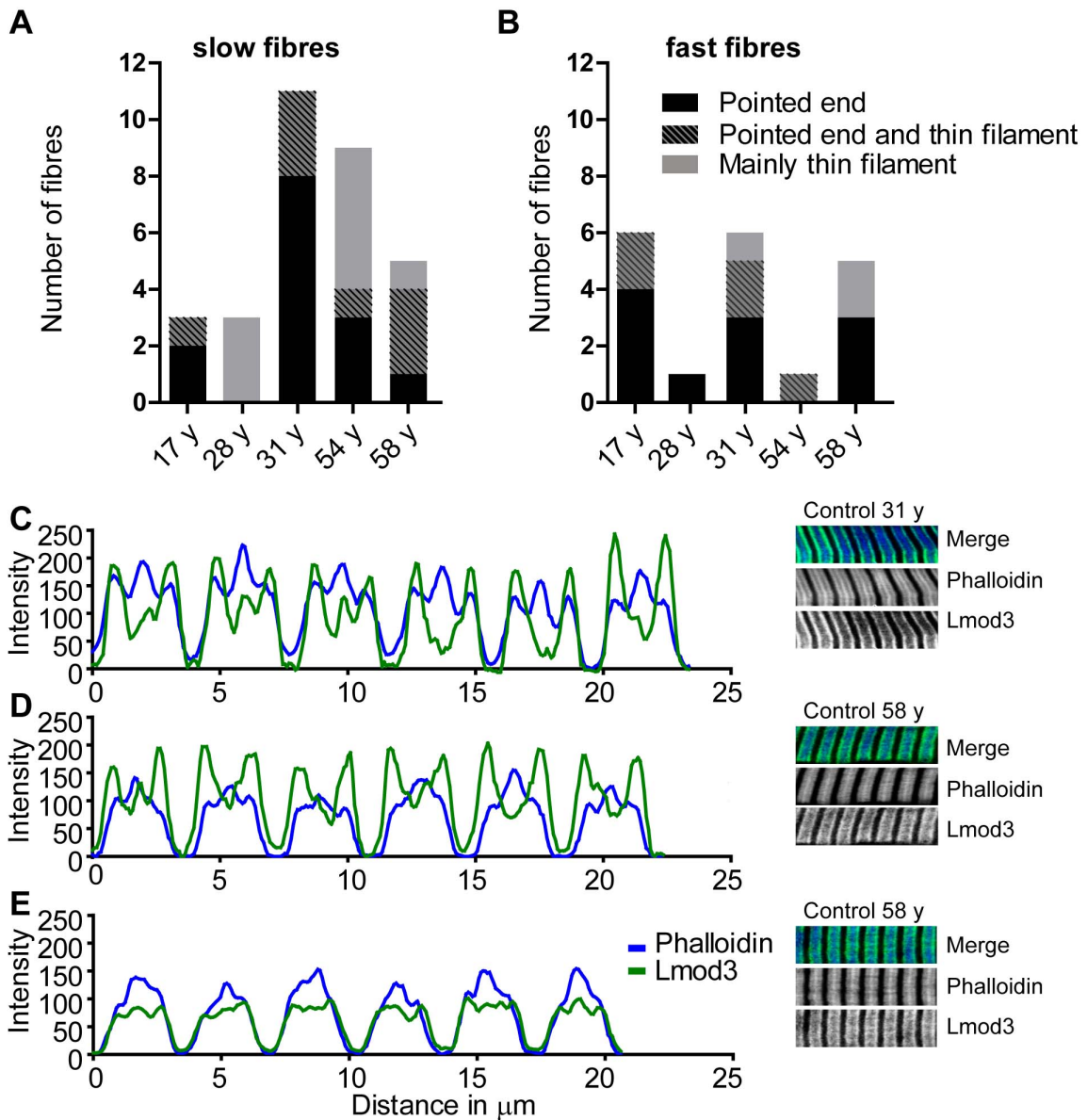
Cultured quail myotubes were either immunolabeled using antibodies against Lmod3 (red) and  $\alpha$ -actinin (green) or transfected with an mCherry-tagged Lmod3 construct (red) and immunolabeled with the  $\alpha$ -actinin Ab (green). In both systems Lmod3 localizes to the centre of the sarcomere (M-line). As these myotubes were unstretched we were not able to resolve the pointed ends from adjacent thin filaments resulting in a single band at the M-line rather than two bands.

Z = Z-disc, P = thin filament pointed end. Scale bar = 2  $\mu$ m



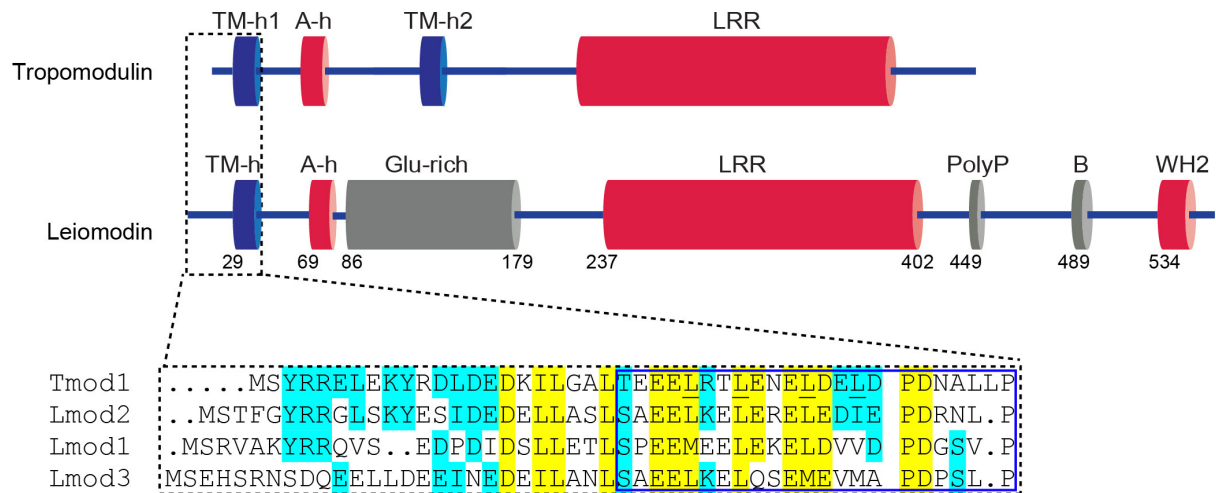
**Supplementary Figure 5: Lmod3 localization in slow and fast muscle fibers**

Examples of Lmod3 localisation in fast and slow fibers, as determined by myosin heavy chain staining, in five control human biopsies. Phalloidin is blue and Lmod3 is green in the merged image. Top row: staining is mostly present near the thin filament pointed end; middle row: staining is present near the pointed end and along the thin filament; bottom row: staining is present mostly along the thin filament. Scale bar: 12.5  $\mu\text{m}$

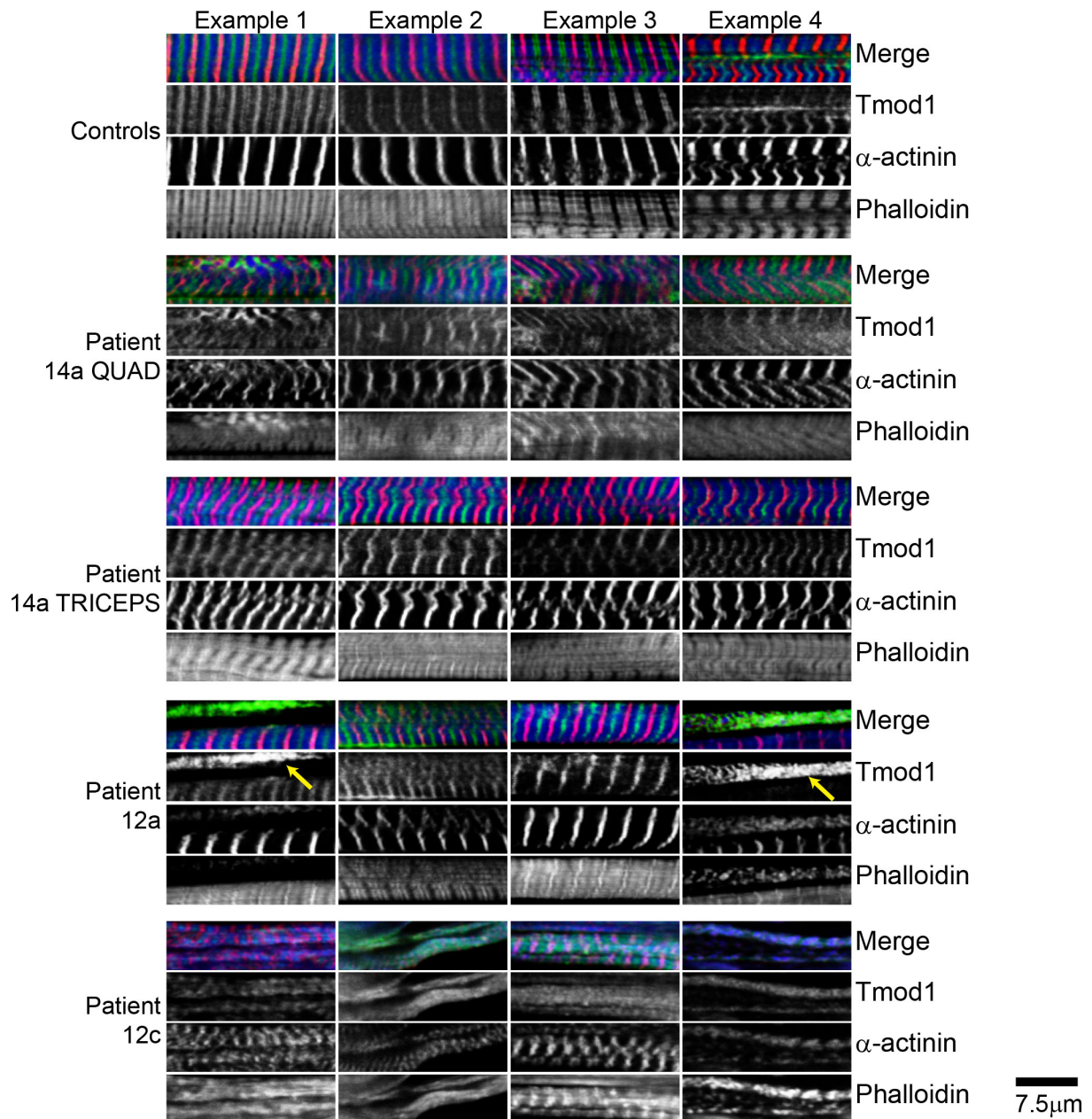


**Supplementary Figure 6: Lmod3 localization in stretched control muscle**

Lmod3 staining pattern in five control muscle biopsies taken between the ages of 17 and 58 years was analyzed in five random areas per biopsy. Myofibers showed one of three staining patterns: (1) staining present mostly near the pointed end (black bars, illustrated in **C**), (2) staining along the thin filament and pointed end (striped bars, illustrated in **D**), (3) staining mostly along the thin filament (gray bars, illustrated in **E**). The fiber type was determined by co-staining with antibodies to the fast and slow myosin heavy chain proteins (MHC). (**A**) Frequency of each pattern in individual biopsies grouped by MHC fiber type. (**C-E**) Profile plot of Lmod3 and phalloidin staining (ImageJ) showing the three staining patterns.

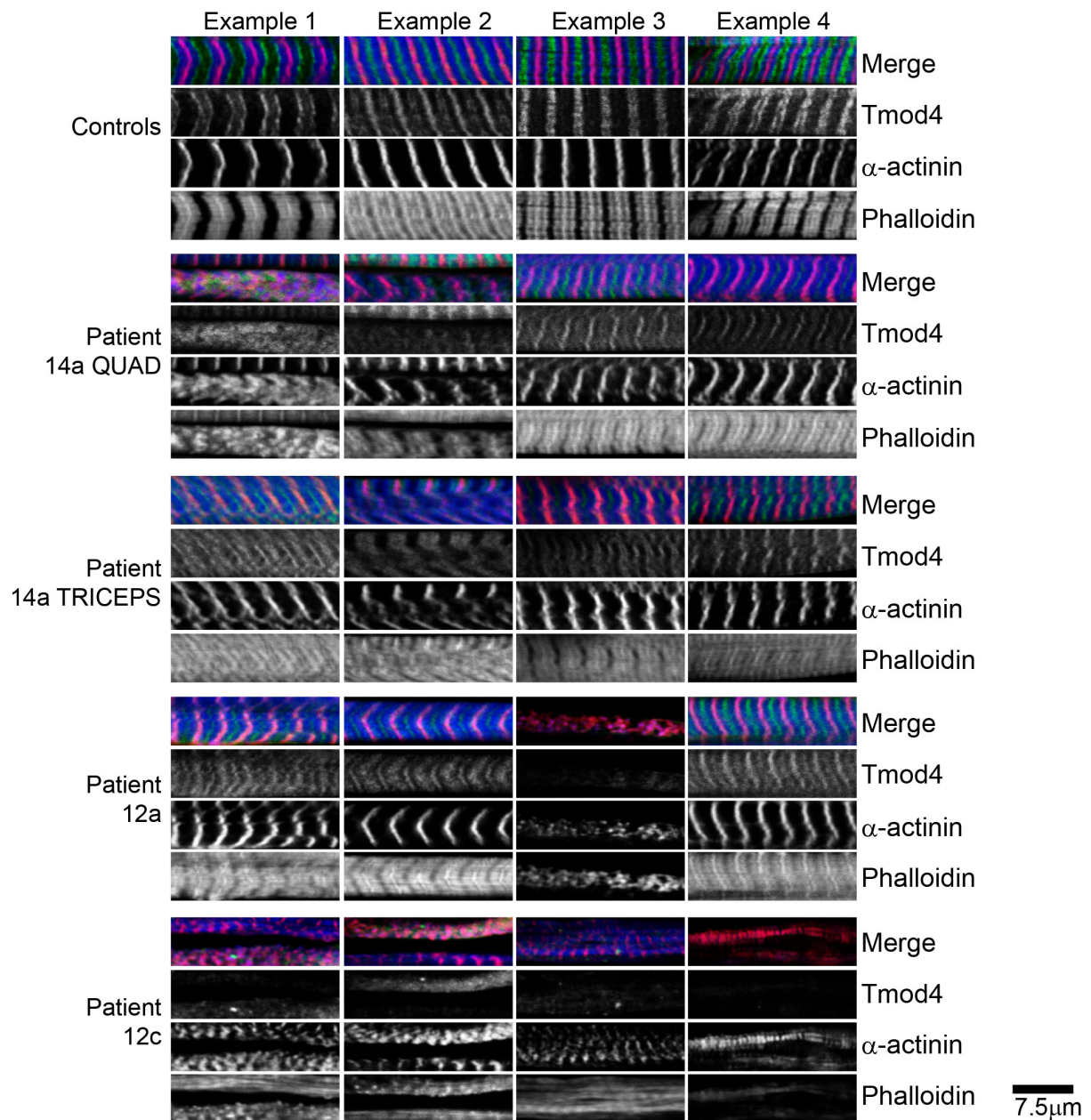


**Supplementary Figure 7: Schematic representation of Tropomodulin (Tmod) and Lmod domain organization and sequence alignment of the shared tropomyosin (TM)-binding domain**  
 Domain organization of Tmod and Lmod showing TM-binding helices (TM-h1, TM-h2), actin binding domains (A-h, LRR, WH2) and areas of unknown function (gray). Below is a sequence alignment of the N-terminal amino acids (indicated by dashed box) including the first TM-binding helix (TM-h1, blue box) shared by all Tmod and Lmod isoforms. The alignment demonstrates that the N-terminal sequence of Lmod3 is more divergent from Tmod1 than Lmod2.



**Supplementary Figure 8: Tmod 1 localization in stretched myofiber bundles from *LMOD3*-NM patients and controls**

Four different regions of Tmod1 staining in three *LMOD3*-NM patient biopsies are shown along with three control muscle samples taken at different ages (example 1-3, taken at ages 28 years, 4 months, 7 days from left to right,) and control mouse tissue (example 4, taken at age 3 days) prepared using the same methods. Co-staining with  $\alpha$ -actinin and phalloidin shows the positions of the z-disc and actin filaments, respectively. Pointed end thin filament localization was observed for Tmod1 in all controls and patients. Due to insufficient stretch the pointed ends from adjacent sarcomeres overlap at the M line and appear as a single band rather than a doublet in most images. Sarcomere and thin filament structure is not well developed in Patient 12c (fetus of 16-17/40 weeks gestation). In Patient 12a, Tmod1 is particularly enriched in fibers that contain amorphous protein accumulations and no discernible sarcomeric structure (yellow arrows). Please note that during the imaging of Tmod1, the gain was adjusted variably to optimally show Tmod1 localization, and therefore differences in signal intensity do not represent differences in expression levels.



**Supplementary Figure 9: Tmod 4 localization in stretched myofiber bundles from *LMOD3*-NM patients and controls**

Four different regions of Tmod4 staining in three *LMOD3*-NM patient biopsies are shown along with three control muscle samples taken at different ages (example 1-3, taken at ages 28 years, 4 months, 7 days from left to right,) and control mouse tissue (example 4, taken at age 3 days) prepared using the same methods. Co-staining with  $\alpha$ -actinin and phalloidin shows the positions of the z-disc and actin filaments, respectively. Pointed end actin filament localization was observed for Tmod4 in all controls and patients. Due to insufficient stretch the pointed ends from adjacent sarcomeres overlap at the M line and appear as a single band rather than as a doublet in most images. Sarcomere and thin filament structure is not well developed in Patient 12c (fetus of 16-17/40 weeks gestation). Tmod4 does not appear enriched in protein accumulations as was observed for Tmod1 (Supplementary figure 8). Please note that during the imaging of Tmod4, the gain was adjusted variably to optimally show Tmod4 localization, and therefore differences in signal intensity do not represent differences in expression levels.

**Supplementary Table 1: Additional genetic testing on *LMOD3*-NM patients**

Family ID	Previous genetic testing for NM
1	<i>NEB</i> – excluded by linkage analysis <i>ACTA1, KBTBD13, KLHL40, TPM2, TPM3, TNNT1</i> - excluded by Sanger sequencing Linkage analysis, homozygosity mapping, whole exome sequencing - no known NM genes were present in linkage regions
2	<i>ACTA1, KBTBD13, KLHL40, NEB, TPM2, TPM3</i> – excluded by Sanger sequencing
3	<i>NEB, TNNT1, TPM3</i> – excluded by Linkage analysis <i>ACTA1, KLHL40, KBTBD13, TPM2</i> - excluded by Sanger sequencing
4	<i>ACTA1, KLHL40</i> – excluded by Sanger sequencing
5	<i>ACTA1, KLHL40</i> – excluded by Sanger sequencing
6	<i>ACTA1, KLHL40, KLHL41</i> – excluded by Sanger sequencing
7	<i>ACTA1, KLHL40</i> – excluded by Sanger sequencing
8	Nemaline myopathy targeted chromosome microarray – no copy number variants found in known NM genes <i>ACTA1, KBTBD13, KLHL40, NEB, TPM2, TPM3</i> - excluded by Sanger sequencing
9	<i>ACTA1, NEB, TPM2, TPM3</i> - excluded by Sanger sequencing
10	<i>ACTA1, KLHL40, NEB, TNNT1, TPM2, TPM3</i> – excluded by Sanger sequencing
11	Nemaline myopathy targeted chromosome microarray – no copy number variants found in known NM genes <i>ACTA1, KBTBD13, NEB, TPM2, TPM3</i> – excluded by Sanger sequencing
12	Whole exome sequencing – no likely pathogenic variants in known NM genes
13	<i>NEB</i> - excluded by linkage analysis <i>ACTA1, KLHL40, TPM2, TPM3</i> - excluded by Sanger sequencing
14	<i>NEB</i> - excluded by linkage analysis <i>ACTA1, TNNT1, TPM2, TPM3</i> – excluded by Sanger sequencing Whole exome sequencing – no likely pathogenic variants found in known NM genes

**Supplementary Table 2: Summary of thin filament structure assessed on phalloidin stained isolated myofiber bundles**

Patient ID	Mutation	Age at Biopsy	Phalloidin staining results <sup>1</sup>
1a	p.S47fs*13	2 d	short thin filaments (1.857±0.3), thick z-discs/short thin filaments (average width = 0.89±0.5)
4	p.W77*	4 m	no sarcomeres
5	p.T101Rfs*4 p.D201Efs*9	2 m	no sarcomeres
6	p.Q117*	10 m	no sarcomeres
7	p.Q117* p.K406Nfs*11	1 yr 7 m	thick z-discs/short thin filaments (average width = 0.64±0.3)
9	p.F287Sfs*3	15 d	no sarcomeres
12a	p.N367Qfs*11	6 wk	normal thin filaments (3.198±0.5), thick z-discs/short thin filaments (average width = N/A)
14a	p.N367del p.R401* Triceps	27 d	regions with normal thin filaments (2.873±0.4), areas of disorganization
14a	p.N367del p.R401* Quadriceps	27 d	regions with normal thin filaments (2.46±0.3), areas of disorganization with short thin filaments (1.228 ± 0.13)
Control biopsies (n=7)		7 d - 31 yr	thin filament length of 2.82± 0.25
<p>m= month, yr= year, d= day, wk= weeks</p> <p><sup>1</sup>Measurements are shown as average width of phalloidin signal (representing two thin filaments) in <math>\mu\text{m} \pm</math> standards deviation of sarcomeres selected based on sufficient stretching from at least 2 separate preparations. This method may overestimate mean thin filament length if filament lengths are variable as the longest filaments are measured and any shorter filaments within the myofiber bundle will be overlooked</p>			

**Supplementary Table 3: LMOD3 sequencing primers**

Primer name	Primer sequence	Product size (bp)
Exon 1-Forward	GTAACTGGGGGACCTTCTTG	488
Exon 1-Reverse	CAAACCCTGGAGTCTTGAG	
Exon 2a-Forward	CTCCACTAGCTGATGCTCCAC	1004
Exon 2a-Reverse	GCTGCTGTTTTGCTCTTCC	
Exon 2b-Forward	CAATCAGAGGCACATGTTGG	692
Exon 2b-Reverse	AGAGAGGGAATAAAGTTGGGATG	
Exon 3-Forward	GCCAGAATTTCAAACCTATTCTG	297
Exon 3-Reverse	TCTGCCTTTTACAAATACCCTTATC	

**References for supplementary information**

1. Abecasis, GR, Auton, A, Brooks, LD, DePristo, MA, Durbin, RM, Handsaker, RE, Kang, HM, Marth, GT, and McVean, GA. 2012. An integrated map of genetic variation from 1,092 human genomes. *Nature* 491:56-65.
2. Chereau, D, Boczkowska, M, Skwarek-Maruszewska, A, Fujiwara, I, Hayes, DB, Rebowski, G, Lappalainen, P, Pollard, TD, and Dominguez, R. 2008. Leiomodins are actin filament nucleators in muscle cells. *Science* 320:239-243.